

Turbulent magnetic decay controlled by two conserved quantities

Axel Brandenburg^{1,2,3,4†} and Aikya Banerjee⁵

¹Nordita, KTH Royal Institute of Technology and Stockholm University, Hannes Alfvéns väg 12, SE-10691 Stockholm, Sweden

²The Oskar Klein Centre, Department of Astronomy, Stockholm University, AlbaNova, SE-10691 Stockholm, Sweden

³McWilliams Center for Cosmology & Department of Physics, Carnegie Mellon University, Pittsburgh, PA 15213, USA

⁴School of Natural Sciences and Medicine, Ilia State University, 3-5 Cholokashvili Avenue, 0194 Tbilisi, Georgia

⁵Department of Physical Sciences, Indian Institute of Science Education and Research Kolkata, Mohanpur 741246, West Bengal, India

(18 June 2024)

The decay of a turbulent magnetic field is slower with helicity than without. Furthermore, the magnetic correlation length grows faster for a helical than a nonhelical field. Both helical and nonhelical decay laws involve conserved quantities: the mean magnetic helicity density and the Hosking integral. Using direct numerical simulations, we show quantitatively that in the fractionally helical case the magnetic energy and correlation length are approximately given by the maximum of the values for the purely helical and purely nonhelical cases. The time of switch-over from one to the other decay law can be obtained on dimensional grounds and is approximately given by $I_H^{1/2} I_M^{-3/2}$, where I_H is the Hosking integral and I_M is the mean magnetic helicity density. An earlier approach based on the decay time is found to agree with our new result and suggests that the Hosking integral exceeds naive estimates by the square of the same resistivity-dependent factor by which the turbulent decay time exceeds the Alfvén time.

Key words: astrophysical plasmas, plasma simulation, plasma nonlinear phenomena

1. Introduction

In recent years, there has been significant interest in the study of decaying turbulent magnetic fields. One of the main applications has been to the understanding of the magnetic field evolution during the radiation-dominated era of early universe (Brandenburg *et al.* 1996; Christensson *et al.* 2001; Banerjee & Jedamzik 2004). The special case with finite magnetic helicity has been studied and understood for a long time (Hatori 1984; Biskamp & Müller 1999). It is the prime example of large-scale magnetic field growth due to an inverse cascade. The possibility of such an inverse cascade is explained by the conservation of magnetic helicity (Frisch *et al.* 1975). However, even in the absence of magnetic helicity, an inverse cascade can develop (Kahniashvili *et al.* 2013; Zrake 2014; Brandenburg *et al.* 2015), and it is well explained by the conservation of what is now called the Hosking integral (Hosking & Schekochihin 2021, 2023a; Zhou *et al.* 2022; Brandenburg *et al.* 2023b), which is the correlation integral of the magnetic helicity density.

† Email address for correspondence: brandenb@nordita.org

In all the cases mentioned above, the spectral magnetic helicity was either zero or it had the same sign at all wavenumbers. A special situation was studied in the work of Brandenburg *et al.* (2023a), where the magnetic helicity was finite, but it was balanced by fermion chirality of the opposite sign, so that the net chirality was vanishing. For such a system, the decay was again successfully explained by the conservation of the Hosking integral, which was adapted to include the chirality from the fermions.

We have seen that the Hosking integral can be applied to broad ranges of systems where magnetic helicity is still important locally, but globally, the net magnetic helicity vanishes. However, there is an important class of astrophysically relevant systems, where the magnetic field is not generated by magnetogenesis, as in the early universe, but by dynamo action. This means that some of the kinetic energy of turbulent motions is converted into magnetic energy. It is important to stress that, even if the velocity field were to be helical, i.e., if there is kinetic helicity in the system, as is generally the case when there is rotation and stratification of density and/or velocity, magnetic helicity conservation still precludes the generation of magnetic helicity, at least on dynamical timescales (Ji 1999).

In the aforementioned helically driven large-scale dynamos, magnetic helicity can be generated at small scales, but it is then balanced by magnetic helicity at large scales so as to conserve magnetic helicity. Alternatively, we can also say that magnetic helicity is produced at large scales, for example by the tilting of buoyantly rising magnetic flux tubes in cyclonic convective events, as envisaged by Parker (1955). Magnetic helicity conservation then implies magnetic twist of opposite sign at smaller scales. In practice, because there is always finite magnetic diffusivity, which acts especially on small scales, the magnetic helicity from large scales will, after some time, dominate the total magnetic helicity owing to the loss at small scales where it has the opposite sign. Therefore, there is always a small imbalance between the contributions from small and large length scales. It is therefore a situation that is only partially suited to the phenomenology involving the conservation of the Hosking integral.

If we now were to turn off the driving, the turbulence would gradually decay. This decay should then be governed by the conservation of both the Hosking integral and the mean magnetic helicity density. This idea is purely theoretical and has never been tested under conditions that we expect to be relevant to astrophysical settings. Such conditions could apply to the decay of a magnetic field produced in a proto-neutron star. There, we expect a turbulent dynamo to occur that is driven by convection (Thompson & Duncan 1993). This would happen when the neutrino opacity is large enough to prevent neutrinos from escaping freely (Epstein 1979; Burrows & Lattimer 1986).

Another source of turbulence in proto-neutron stars could be the magnetorotational instability that results from the radially outward decreasing angular velocity gradient associated with collapsed material having an approximately constant angular momentum density (Guilet *et al.* 2022). In both cases, the turbulence itself has kinetic helicity of opposite signs in the northern and southern hemispheres (negative in the north and positive in the south). In each hemisphere, this leads to dynamo action of the type described above, but the magnetic helicities have opposite signs not only in the two hemispheres, but also on small and large length scales. One would thus focus only on one hemisphere and ignore the interaction between north and south. The magnetic helicities from small and large length scales would then nearly cancel. Such fields have been called “bihelical” and their decay properties were first studied by Yousef & Brandenburg (2003). They found that the positive and negative contributions rapidly mix and annihilate and that the ratio of the magnetic helicity spectrum to the magnetic energy spectrum has

local extrema both at small and large scales, although the latter is dominant in an absolute sense.

Since the net magnetic helicity of a bihelical magnetic field does not vanish exactly, and since the mean magnetic helicity itself is an important conserved quantity, we are confronted with a situation where the magnetic decay is governed by two conserved quantities. Investigating this aspect in a more controlled fashion is the main purpose of this paper.

In an earlier paper, Tevzadze *et al.* (2012) did already study a case with fractional helicity. They found that the correlation length developed a steeper growth (indicative of magnetic helicity domination) at a specific moment that depends on the value of the magnetic helicity as well as on the initial values of the magnetic energy and the magnetic correlation length.

Meanwhile, we know about the Hosking integral I_H and can ask whether the time of switch-over from a decay controlled by I_H to one controlled by the mean magnetic helicity density I_M can be computed based on dimensional arguments. Indeed, given that the quantity I_H has dimensions $\text{cm}^9 \text{s}^{-4}$ and I_M has dimensions $\text{cm}^3 \text{s}^{-2}$ (see Brandenburg 2023, and note that the magnetic field is here understood to be in Alfvén units with dimensions cm s^{-1}), a combination of I_H and I_M that yields a time would be $I_H^{1/2} I_M^{-3/2}$. It will turn out that this is indeed the time of switch-over between the two regimes.

2. Our model

2.1. Basic equations

We simulate the compressible magnetohydrodynamic (MHD) equations with an isothermal equation of state with constant sound speed c_s , so the pressure p and the density ρ are related by $p = \rho c_s^2$. The equations for the magnetic vector potential, \mathbf{A} , the velocity \mathbf{U} , and the logarithmic density $\ln \rho$, are

$$\frac{\partial \mathbf{A}}{\partial t} = \mathbf{U} \times \mathbf{B} + \eta \nabla^2 \mathbf{A}, \quad (2.1)$$

$$\frac{D\mathbf{U}}{Dt} = \mathbf{f} - c_s^2 \nabla \ln \rho + \frac{1}{\rho} [\mathbf{J} \times \mathbf{B} + \nabla \cdot (2\rho \nu \mathbf{S})], \quad (2.2)$$

$$\frac{D \ln \rho}{Dt} = -\nabla \cdot \mathbf{U}, \quad (2.3)$$

where $D/Dt = \partial/\partial t + \mathbf{U} \cdot \nabla$ is the advective derivative, $\mathbf{B} = \nabla \times \mathbf{A}$ is the magnetic field, $\mathbf{J} = \nabla \times \mathbf{B}/\mu_0$ is the current density, μ_0 is the vacuum permeability, ν is the viscosity, $S_{ij} = (\partial_i U_j + \partial_j U_i)/2 - \delta_{ij} \nabla \cdot \mathbf{U}/3$ are the components of the traceless rate-of-strain tensor \mathbf{S} , and \mathbf{f} is a monochromatic, spatially periodic forcing function with wavenumber k , where $k = |\mathbf{k}|$ is the length of the wavevector that is taken randomly at each time step from a shell of thickness δk such that $k_f - \delta k/2 \leq k < k_f + \delta k/2$ with k_f being the mean forcing wavenumber. Our computational domain is a periodic cube of size L^3 , and $k_1 = 2\pi/L$ is the smallest wave number.

2.2. Parameters of the model

The amplitude f_0 of the forcing function is chosen such that the rms velocity u_{rms} is about 10% of the sound speed. The system is governed by the rms Mach number as well as the kinetic and magnetic Reynolds numbers,

$$\text{Ma} = u_{\text{rms}}/c_s, \quad \text{Re} = u_{\text{rms}}/\nu k_f, \quad \text{Re}_M = u_{\text{rms}}/\eta k_f. \quad (2.4)$$

When the value of Re_M is sufficiently large, there is dynamo action, i.e., the rms magnetic field strength, B_{rms} , increases exponentially. The initial magnetic field is chosen to be a random, Gaussian-distributed field of sufficiently low amplitude so that B_{rms} grows initially exponentially before it saturates at a value that is comparable to the equipartition field strength $B_{\text{eq}} = \sqrt{\rho_0 \mu_0} u_{\text{rms}}$.

To recover information about the turbulent decay that is independent of the size and shape of the computational domain, we must choose the value of k_f/k_1 to be sufficiently large. The sensitivity of this on the results has been studied on various occasions (e.g., Zhou *et al.* 2022). A reasonable compromise that still allows for sufficiently large Reynolds numbers seems to be $k_f/k_1 = 60$. This is the value that will be used for the main run in the present paper, but we also present some results with $k_f/k_1 = 30$.

2.3. Initial conditions

So far, the model is equivalent to that of Brandenburg (2001), who studied the large-scale dynamo action associated with helical turbulence. The new aspect is that we now also simulate the case where the turbulent driving is turned off, i.e., $f_0 = 0$. In those cases, we use as initial condition a snapshot from the driven simulation at a time when the magnetic field has still not yet reached saturation, i.e., the magnetic field is still in the kinematic regime. In the more idealized studies where we focus on the decay governed by two conserved quantities (Hosking integral and mean magnetic helicity density), we construct an initial magnetic vector potential in Fourier space as $\hat{\mathbf{A}}(\mathbf{k}) = \mathbf{R}(\mathbf{k}; \varsigma) \hat{\mathbf{A}}^{\text{nhel}}$, where

$$\mathbf{R}_{ij}(\mathbf{k}; \varsigma) = \delta_{ij} - \hat{k}_i \hat{k}_j + i \hat{k}_\ell \varsigma \epsilon_{ij\ell} \quad (2.5)$$

is a matrix with \hat{k}_i being the components of the unit vector $\hat{\mathbf{k}} = \mathbf{k}/k$, $|\varsigma| \leq 1$ is a nondimensional parameter that quantifies the fractional helicity, and $\hat{\mathbf{A}}^{\text{nhel}}$ is a nonhelical field with random phases and possesses the desired spectrum for the magnetic field $\text{Sp}(\mathbf{B}) = k^2 \text{Sp}(\mathbf{A})$, i.e.,

$$\text{Sp}(\mathbf{B}) = \frac{A_0 k^\alpha}{1 + (k/k_p)^{5/3+\alpha}}, \quad (2.6)$$

where A_0 is an amplitude, k_p denotes the initial position of the spectral peak, α is the subinertial range slope (usually $\alpha = 4$), and the inertial range has a $k^{-5/3}$ spectrum. For $\varsigma \neq 0$, we have a finite magnetic helicity and expect them the decay to be governed by both the Hosking integral and the mean magnetic helicity density.

In Eq. (2.6), $\text{Sp}(\cdot)$ denotes a shell integrated spectrum. This operation will also be applied to the local, gauge-dependent magnetic helicity density $h = \mathbf{A} \cdot \mathbf{B}$, so that $\text{Sp}(h) = (k^2/8\pi^3 L^3) \int_{4\pi} |\tilde{h}|^2 d\Omega_k$. The tilde marks a quantity in Fourier space, and Ω_k is the solid angle in Fourier space, so that $\int \text{Sp}(h) dk = \langle h^2 \rangle$, and likewise for $\int \text{Sp}(\mathbf{B}) dk = \langle \mathbf{B}^2 \rangle$. Owing to the integration over shells in three-dimensional wavenumber space, the spectrum of a spatially random (δ correlated) field is proportional to k^2 . This is indeed the case for a globally non-helical field, where $\langle h \rangle = 0$.

2.4. Diagnostic parameters

The relevant information that quantifies the Hosking integral is the first nonvanishing coefficient in the Taylor expansion,

$$\text{Sp}(h)|_{k \rightarrow 0} = \frac{I_H}{2\pi^2} k^2 + \dots; \quad (2.7)$$

see Hosking & Schekochihin (2021), Schekochihin (2022), and Zhou *et al.* (2022) for details. This is also the method used here to determine the value of I_H . We confirm

that $2\pi^2\text{Sp}(h)/k^2$ has a flat part for small values of k and use its value at $k = k_1$ to measure I_H . Below, we also confirm that I_H is nearly independent of time; Zhou *et al.* (2022) for quantitative assessment of its invariance in the ideal limit. Note also that, since $\int \text{Sp}(h) dk = \langle h^2 \rangle$, which has dimensions $(\text{cm}^3 \text{s}^{-2})^2$, $\text{Sp}(h)$ has dimensions, $\text{cm}^7 \text{s}^{-4}$ and therefore I_H has dimensions $\text{cm}^9 \text{s}^{-4}$, as expected.

Our model is spatially homogeneous and we consider in all cases periodic boundary conditions. The model can then be characterized by the magnetic energy and helicity spectra, $E_M(k, t)$ and $H_M(k, t)$, respectively. They are normalized such that their integrals give the mean magnetic energy and helicity densities, $\mathcal{E}_M \equiv \int E_M(k, t) dk = \langle \mathbf{B}^2 \rangle / 2\mu_0$ and $I_M \equiv \int H_M(k, t) dk = \langle \mathbf{A} \cdot \mathbf{B} \rangle$, respectively.† Here and below, angle brackets denote volume averaging.

The position of the peak of the spectrum is characterized by the inverse magnetic integral scale, $k_{\text{peak}} = \xi_M^{-1}$, where ξ_M is here defined as

$$\xi_M = \int k^{-1} E_M(k, t) dk \bigg/ \int E_M(k, t) dk. \quad (2.8)$$

Of particular importance are the time dependencies $\xi_M(t)$ and $\mathcal{E}_M(t)$, which, in turn, are characterized by the instantaneous scaling exponents $q(t) = d \ln \xi_M / d \ln t$ and $p(t) = -d \ln \mathcal{E}_M / d \ln t$.

To facilitate comparison with other work, it is useful to present our results in nondimensional form. The time used in the numerical simulations is made nondimensional by plotting the evolution versus $c_s k_1 t$, which is convenient for numerical reasons, because c_s and k_1 are constant in time. However, physically more meaningful would be a nondimensionalization by using the Alfvén speed and the inverse correlation length. Both are time dependent, but the values v_{Ae} and k_e at the end of the simulations seem to be most meaningful.

3. Results

In the present context, we have to deal with two conserved quantities, namely the Hosking integral I_H and the mean magnetic helicity density $I_M = \langle \mathbf{A} \cdot \mathbf{B} \rangle$. The former case has been studied extensively in recent years. Specifically, Brandenburg & Larsson (2023) and Brandenburg *et al.* (2023b) found

$$\xi_M(t) \approx 0.12 I_H^{1/9} t^{4/9}, \quad \mathcal{E}_M(t) \approx 3.7 I_H^{2/9} t^{-10/9}, \quad E_M(k, t) \lesssim 0.025 I_H^{1/2} (k/k_0)^{3/2}. \quad (3.1)$$

The hope is that the coefficients in these expressions are universal, but it should be noted that they have not yet been verified in other contexts.

3.1. Decay controlled by magnetic helicity

In the helical case with $I_M \neq 0$, we have $\xi_M \propto t^{2/3}$ and $\mathcal{E}_M \propto t^{-2/3}$ (Hatori 1984; Biskamp & Müller 1999; Brandenburg & Kahniashvili 2017). In the present context, the pre-factors are important. Using the data from Fig. 2(c) of Brandenburg & Kahniashvili (2017), we find

$$\xi_M(t) \approx 0.12 I_M^{1/3} t^{2/3}, \quad \mathcal{E}_M(t) \approx 4.3 I_M^{2/3} t^{-2/3}, \quad E_M(k, t) \lesssim 0.7 I_M. \quad (3.2)$$

† The name I_M has been chosen here to mark its important role as an ideal invariant and to highlight its usage analogously with that of the Hosking integral I_H .

TABLE 1. Summary of the coefficients characterizing the decays governed by the conservation of magnetic helicity ($i = M$) and the Hosking integral ($i = H$).

i	β	q	p	σ	$C_i^{(\xi)}$	$C_i^{(\mathcal{E})}$	$C_i^{(E)}$
M	0	2/3	2/3	1/3	0.13	4.1	0.7
H	3/2	4/9	10/9	1/9	0.12	3.7	0.025

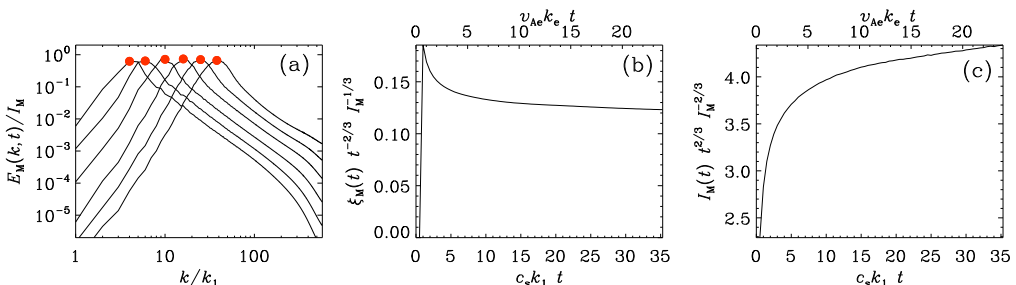


FIGURE 1. (a) Magnetic energy spectra, as well as compensated evolutions of (b) $\xi_M(t)$ and (c) $\mathcal{E}_M(t)$ for the maximally helical run of Fig. 2(c) of Brandenburg & Kahnishvili (2017). In (a), the red symbols denote the spectral peaks.

Generally, we can write

$$\xi_M(t) = C_i^{(\xi)} I_i^\sigma t^q, \quad \mathcal{E}_M(t) = C_i^{(\mathcal{E})} I_i^{2\sigma} t^{-p}, \quad E_M(k) = C_i^{(E)} I_i^{(3+\beta)\sigma} (k/k_0)^\beta, \quad (3.3)$$

where the index i in the integrals I_i and the coefficients $C_i^{(\xi)}$, $C_i^{(\mathcal{E})}$, and $C_i^{(E)}$ stand for M or H for magnetic helicity and Hosking scalings, respectively, and σ is the exponent with which length enters in I_i : $\sigma = 1/3$ for the magnetic helicity density ($i = M$) and $\sigma = 1/9$ for the Hosking integral ($i = H$); see Table 1 for a summary of the coefficients.†

In Figure 1, we show the magnetic energy spectra, as well as compensated evolutions of $\xi_M(t)$ and $\mathcal{E}_M(t)$ for the maximally helical run of Fig. 2(c) of Brandenburg & Kahnishvili (2017). We see that the peak of $\mathcal{E}_M(t)$ remains underneath a nearly flat envelope (its slope is $\beta = 0$), as is expected for a fully helical turbulent decay. Although the compensated evolutions of $\xi_M(t)$ and $\mathcal{E}_M(t)$ are not yet fully converged toward the end of that run (the lines are now yet flat), we can already read off the approximate values $C_M^{(\xi)} \approx 0.12$ and $C_M^{(\mathcal{E})} \approx 4.3$ toward the end of the run. The values of these coefficients will be revisited later in this paper.

In Figure 2, we again show the compensated evolutions of $\xi_M(t)$ and $\mathcal{E}_M(t)$, but now for a nearly perfectly nonhelical new run ($\varsigma = 0.003$) with $k_f/k_1 = 30$. The resulting values coefficients are close to those estimated previously, namely $C_H^{(\xi)} \approx 0.12$ and $C_H^{(\mathcal{E})} \approx 4.7$. This supports the previous hypotheses of Brandenburg & Larsson (2023) and Brandenburg *et al.* (2023b) that these coefficients may indeed be universal.

To determine the value of $I_H(t)$, we plot in Figure 3 the evolutions of $(2\pi^2/k^2) \text{Sp}(h)$ (normalized by v_{Ae}^4/k_e^5) for $k/k_1 = 1, 2$, and 3 for the run with $k_f/k_1 = 30$ and $\varsigma = 0.003$.

† In Eq. (3.3c), we have here corrected a typo in Eq. (12c) of Brandenburg & Larsson (2023) and Eq. (3.1c) of Brandenburg *et al.* (2023b), where the exponent on I_i was incorrectly stated as $(3 + \beta)/\sigma$ instead of $(3 + \beta)\sigma$, but the calculations were done correctly.

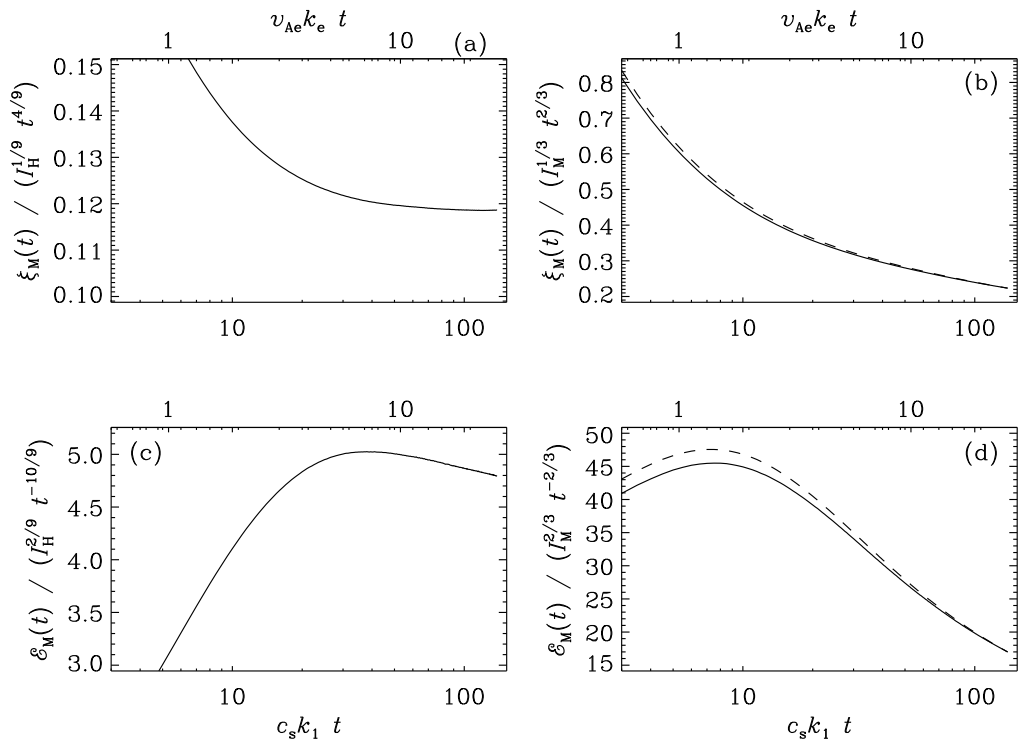


FIGURE 2. Evolution of $\xi_M(t)$ (upper row) and $\mathcal{E}_M(t)$ (lower row) for the run with $k_f/k_1 = 30$ and $\zeta = 0.003$, compensated by the expected evolution if the decay is controlled either by I_H (left column) or by I_M (right column). The dashed line denotes the use of I_M at the end of the run, while for the solid line, the time-dependent value was taken.

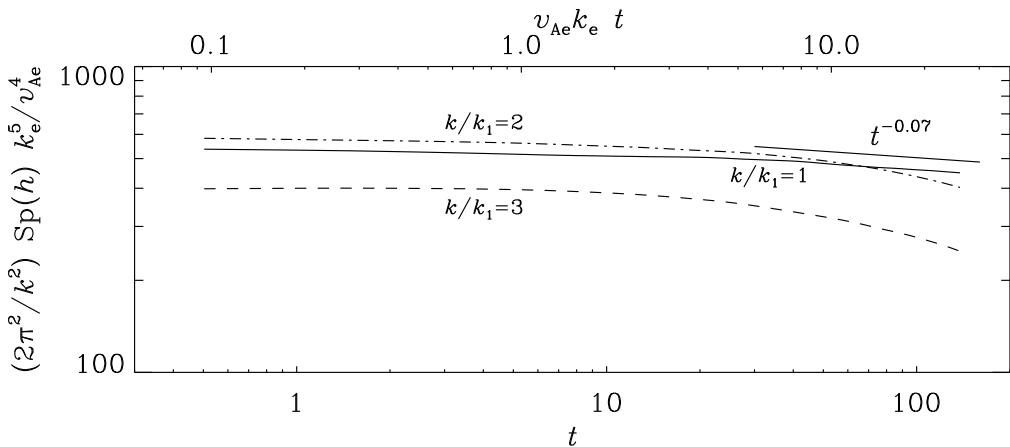


FIGURE 3. Evolutions of $(2\pi^2/k^2) \text{Sp}(h)$, normalized by v_{Ae}^4/k_e^5 , for $k/k_1 = 1$ (solid line), 2 (dashed-dotted line), and 3 (dashed line), for the nearly nonhelical run with $\zeta = 0.003$ and $k_f/k_1 = 30$.

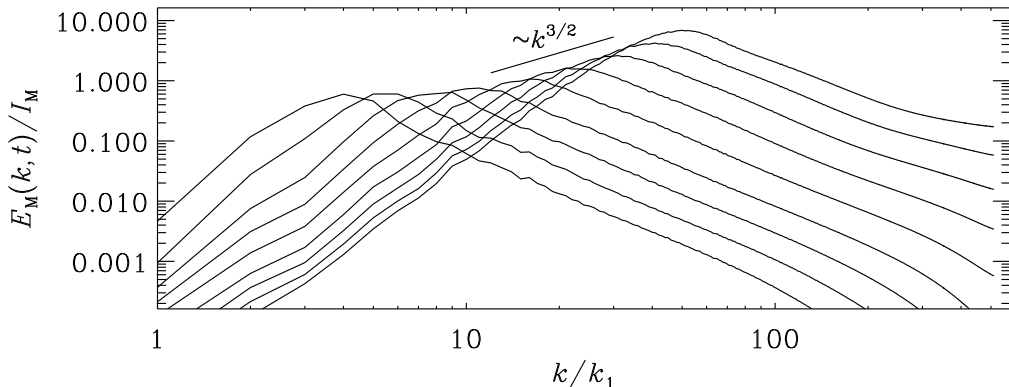


FIGURE 4. Magnetic energy spectra for $k_f/k_1 = 60$ and $\zeta = 0.01$ at times $v_{Ae}k_e t = 0.07, 0.18, 0.40, 0.82, 1.65, 3.3, 6.1, 11.1,$ and 20.7 .

We see that for $k/k_1 = 1$, the result shows a nearly negligible decline proportional to $t^{0.07}$. Note that, in units of v_{Ae}^4/k_e^5 , the value of I_H is about 500.

3.2. Decay controlled by I_M and I_H

If both I_M and I_H control the decay, we have a combination of the two decay laws such that the late times are always controlled by the more strongly conserve quantity, i.e., by I_M , so

$$\xi_M \approx 0.12 I_M^{1/3} t^{2/3} + 0.12 I_H^{1/9} t^{4/9}, \quad (3.4)$$

$$\mathcal{E}_M \approx 4.3 I_M^{2/3} t^{-2/3} + 3.7 I_H^{2/9} t^{-10/9}. \quad (3.5)$$

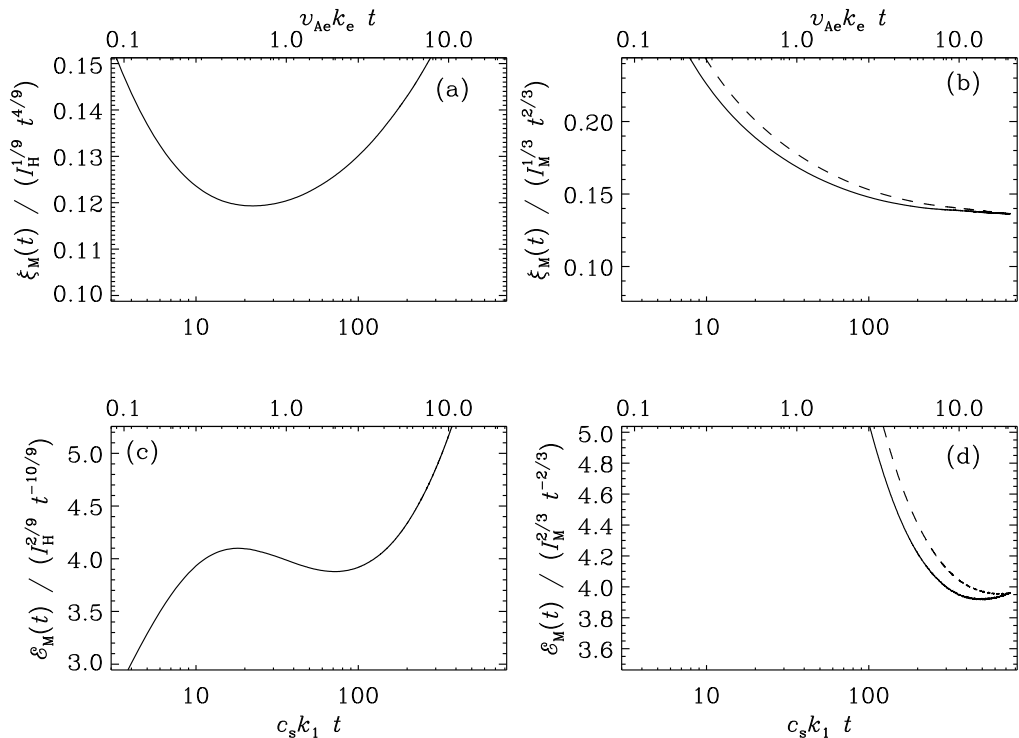
Since the second term involving I_H is initially larger, one expects their contributions to be dominant after some time. Thus, the magnetic helicity will always survive and be the dominant contributed to explaining the decay.

To examine now a run where the decay is controlled both by I_M and I_H , we now increase the initial fractional helicity slightly from 0.003 to 0.01; see Figure 4 for magnetic energy spectra at different times for a run with $k_f/k_1 = 60$ and $\zeta = 0.01$. Note that the peaks of the spectra evolve at first underneath an envelope with the slope $\beta = 3/2$, as expected for a decay controlled by I_H . At later times, however, the envelope becomes flat (slope $\beta = 0$), as expected for a decay controlled by I_M . I_H .

In Figure 5, we show the evolutions of $\xi_M(t)$ and $\mathcal{E}_M(t)$ for $k_f/k_1 = 60$ and $\zeta = 0.01$ compensated by $t^{-2/3}$ and $t^{2/3}$, respectively, as well as $t^{-4/9}$ and $t^{10/9}$, respectively. We see that now the curves compensated by $t^{-2/3}$ and $t^{2/3}$, respectively, become nearly constant, as expected for a decay that is governed by magnetic helicity conservation. Specifically, we find $\xi_M/(I_M^{1/3} t^{2/3}) \approx 0.14$ and $\mathcal{E}_M/(I_M^{2/3} t^{-2/3}) \approx 4.0$. During a short intermediate interval, however, we see that the curves compensated by $t^{-4/9}$ and $t^{10/9}$, respectively, show brief plateaus around $v_{Ae}k_e t = 1$ with $\xi_M/(I_H^{1/9} t^{4/9}) \approx 0.12$ and $\mathcal{E}_M/(I_H^{2/9} t^{-10/9}) \approx 4.0$.

3.3. Improved fits with I_M and I_H

We have seen that the limiting cases where the decay is controlled either by I_M or by I_H are well reproduced by Eq. (3.3). It turns out, however, that the combined fits given by Eqs. (3.4) and (3.5) are not very accurate. Improved fits can be obtained by using


 FIGURE 5. Similar to Figure 2, but for $k_t/k_1 = 60$ and $\zeta = 0.01$.

large weighting exponents for both contributions, i.e.,

$$\xi_M \approx \left[\left(0.12 I_M^{1/3} t^{2/3} \right)^q + \left(0.14 I_H^{1/9} t^{4/9} \right)^q \right]^{1/q}, \quad (3.6)$$

$$\mathcal{E}_M \approx \left[\left(4.0 I_M^{2/3} t^{-2/3} \right)^q + \left(4.0 I_H^{2/9} t^{-10/9} \right)^q \right]^{1/q}. \quad (3.7)$$

The result is shown in Figure 6, where we show that $q = 10$ yields satisfactory fits, while $q = 2$ and $q = 1$ (our original hypothesis) are poor. The fact that the coefficients for both parts are different from those of the individual fits and that they happen to be 4.0 in Eq. (3.7), but different from each other in Eq. (3.6) is probably just by chance and reflect that degree of uncertainty of these values.

It is important to emphasize that the limit $q \rightarrow \infty$ corresponds to

$$\xi_M \approx \max \left(0.12 I_M^{1/3} t^{2/3}, 0.14 I_H^{1/9} t^{4/9} \right), \quad (3.8)$$

$$\mathcal{E}_M \approx \max \left(4.0 I_M^{2/3} t^{-2/3}, 4.0 I_H^{2/9} t^{-10/9} \right). \quad (3.9)$$

These expressions yield discontinuities in the derivative. An advantage of such expressions is that one can clearly see the regimes of validity of both expressions. The critical times when characterizing the cross-over from Hosking scaling to magnetic helicity scaling are given by

$$t_\xi \approx (0.12/0.14)^{9/2} (I_H/I_M^3)^{1/2} \approx 0.50 I_H^{1/2} I_M^{-3/2}, \quad (3.10)$$

$$t_\mathcal{E} \approx I_H^{1/2} I_M^{-3/2}. \quad (3.11)$$

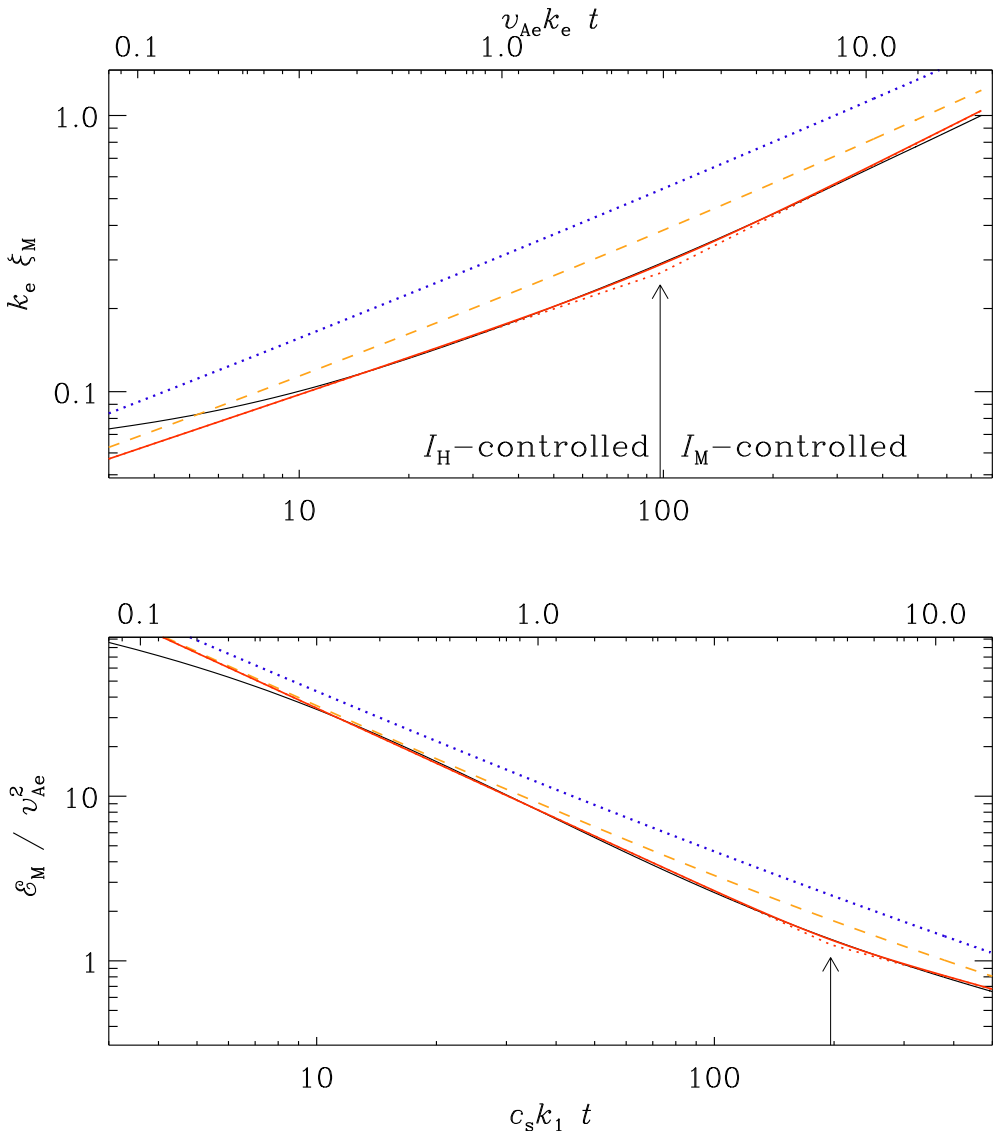


FIGURE 6. Decay of magnetic energy (black line) and the fit given by Eq. (3.5) (dotted blue line) as well as Eq. (3.7) with $q = 2$ (dashed orange line) and $q = 10$ (red). The red dotted line corresponds to the limit $q \rightarrow \infty$, as realized by Eqs. (3.8) and (3.9).

It would be plausible to assume that both times should equal each other. The fact that they are not equal to each other might hint, again, at the possibility that the precise values of these coefficients are still uncertain. On the other hand, looking at Figure 5, it is actually true that ξ_M approaches the I_M -dominated scaling by a factor two earlier than \mathcal{E}_M .

3.4. Comparison with earlier work

As mentioned in the introduction, the switch-over time from nonhelicity to helicity dominated decay has been studied by Tevzadze *et al.* (2012) under the assumption that $p = 1$ and $q = 1/2$ (Christensson *et al.* 2001) instead of $p = 10/9$ and $q = 4/9$, as

now motivated by the conservation of the Hosking integral. The basic idea is to assume that at the time of switch-over, t_* , the real-space realizability condition (Biskamp 2003; Kahniashvili *et al.* 2010) is saturated, i.e., $2\xi_M(t_*)\mathcal{E}_M(t_*) = I_M$. Next, inserting $\xi_M(t_*) = \xi_M(t_0)(t_*/t_0)^q$ and $\mathcal{E}_M(t_*) = \mathcal{E}_M(t_0)(t_*/t_0)^{-p}$, we find $2\xi_M(t_0)\mathcal{E}_M(t_0)(t_*/t_0)^{-(p-q)} = I_M$, and therefore

$$t_* = t_0 [2\xi_M(t_0)\mathcal{E}_M(t_0)/I_M]^{1/(p-q)}. \quad (3.12)$$

For $p = 1$ and $q = 1/2$, we have $1/(p - q) = 2$ and recover the result of Tevzadze *et al.* (2012), while for $p = 10/9$ and $q = 4/9$, we have $1/(p - q) = 3/2$. Comparing with Eq. (3.11), we see that I_M enters with the same exponent $3/2$, and that the remainder can be identified with

$$I_H = [2\xi_M(t_0)\mathcal{E}_M(t_0)]^3 t_0^2. \quad (3.13)$$

This suggests that I_H is related to ξ_M and \mathcal{E}_M , but the problem is that t_0 is not straightforwardly related to the Alfvén time ξ_M/v_A , where $v_A^2 = 2\mathcal{E}_M$. Indeed, Brandenburg *et al.* (2024) found that there is a pre-factor C_M that increases with increasing magnetic Reynolds number. Thus, inserting $t = C_M\xi_M/v_A$, we find

$$I_H = C_M^2 \xi_M^5 v_A^4. \quad (3.14)$$

The facts that C_M enters quadratically and approaches values in the range 20–50 for large magnetic Reynolds numbers explains why I_H strongly exceeds the naive estimate $\xi_M^5 v_A^4$. Interestingly, Zhou *et al.* (2022) found that part of the large excess over the naive estimate is related to non-Gaussianity. Another smaller part has to do with the spectral shape. Linking the value of C_M to non-Gaussianity provides a new clue to the question of why there is a resistivity-dependent relation between decay and Alfvén times in hydromagnetic turbulence.

4. Conclusions

The present work has shown that the decay laws for the combined case of two conserved quantities is best represented not simply by the sum of the individual laws, but that a good description of the numerical results is obtained by taking the maximum between the two individual decay laws. The switch-over from one to the other decay law occurs earlier for $\xi_M(t)$ than for $\mathcal{E}_M(t)$. This behavior is surprising, but also confirmed by direct inspection of the two time traces in Figure 5(b) and (d).

Comparing with earlier work on the switch-over from one to the other regime suggests that the decay time enters in such a relation. This is remarkable, because in hydromagnetic turbulence the decay time is known to be longer than the Alfvén time by a resistivity-dependent factor of up to 50. This property might also explain why the value of the Hosking integral is always found to strongly exceed the naive estimate $\xi_M^5 v_A^4$. However, as shown in Zhou *et al.* (2022), also other factors enter that involve the spectral shape. It would therefore be interesting to revisit this question.

As alluded to in the introduction, an obvious astrophysical application of our work is the decay of an initially bihelical magnetic field. Such situations are important in proto-neutron stars after the neutrino-driven convection ceases. Although this was actually our initial motivation, we have not analyzed this case any further, because the most important aspect turned out to be the fact that the magnetic field has always fractional helicity in such cases, which we have now addressed.

A more general question is that of a decay governed by two decay laws and whether there are other useful examples where the physics discussed in the present paper can be studied. As far as turbulence is concerned, one might think of the Loitsyansky and

Saffman integrals, which represent the coefficients of the k^4 and k^2 terms in the Taylor expansion of the kinetic energy spectrum (see, e.g., Davidson 2000). Here, the Saffman integral might become more important at later times when long-range interactions have occurred (Hosking & Schekochihin 2023*b*). This could also be applied to the magnetic case.

Funding

This work was supported in part by the Swedish Research Council (Vetenskapsrådet, 2019-04234), the National Science Foundation under Grant No. NSF PHY-2307698, and a NASA ATP Award 80NSSC22K0825. We acknowledge the inspiring atmosphere during the program on the “Generation, evolution, and observations of cosmological magnetic fields” at the Bernoulli Center in Lausanne. We acknowledge the allocation of computing resources provided by the Swedish National Allocations Committee at the Center for Parallel Computers at the Royal Institute of Technology in Stockholm and Linköping.

Declaration of Interests

The authors report no conflict of interest.

Data availability statement

The data that support the findings of this study are openly available on <http://norlrx65.nordita.org>. All calculations have been performed with the PENCIL CODE (Pencil Code Collaboration *et al.* 2021); DOI:10.5281/zenodo.3961647.

Authors’ ORCIDs

A. Brandenburg, <https://orcid.org/0000-0002-7304-021X>

A. Banerjee, <https://orcid.org/0009-0004-6288-0362>

REFERENCES

- BANERJEE, R. & JEDAMZIK, K. 2004 Evolution of cosmic magnetic fields: From the very early universe, to recombination, to the present. *Phys. Rev. D* **70**, 123003.
- BISKAMP, DIETER 2003 *Magnetohydrodynamic Turbulence*. Cambridge, UK: Cambridge University Press.
- BISKAMP, D. & MÜLLER, W.-C. 1999 Decay Laws for Three-Dimensional Magnetohydrodynamic Turbulence. *Phys. Rev. Lett.* **83** (11), 2195–2198, arXiv: physics/9903028.
- BRANDENBURG, A. 2001 The Inverse Cascade and Nonlinear Alpha-Effect in Simulations of Isotropic Helical Hydromagnetic Turbulence. *Astrophys. J.* **550** (2), 824–840, arXiv: astro-ph/0006186.
- BRANDENBURG, A. 2023 Hosking integral in non-helical Hall cascade. *J. Plasma Phys.* **89** (1), 175890101, arXiv: 2211.14197.
- BRANDENBURG, A., ENQVIST, K. & OLESEN, P. 1996 Large-scale magnetic fields from hydromagnetic turbulence in the very early universe. *Phys. Rev. D* **54** (2), 1291–1300, arXiv: astro-ph/9602031.
- BRANDENBURG, A. & KAHNIASHVILI, T. 2017 Classes of Hydrodynamic and Magnetohydrodynamic Turbulent Decay. *Phys. Rev. Lett.* **118**, 055102, arXiv: 1607.01360.
- BRANDENBURG, A., KAHNIASHVILI, T. & TEVZADZE, A. G. 2015 Nonhelical inverse transfer of a decaying turbulent magnetic field. *Phys. Rev. Lett.* **114** (7), 075001, arXiv: 1404.2238.
- BRANDENBURG, A., KAMADA, K. & SCHOBER, J. 2023*a* Decay law of magnetic turbulence with helicity balanced by chiral fermions. *Phys. Rev. Res.* **5** (2), L022028, arXiv: 2302.00512.

- BRANDENBURG, A. & LARSSON, G. 2023 Turbulence with Magnetic Helicity That Is Absent on Average. *Atmosphere* **14** (6), 932, arXiv: 2305.08769.
- BRANDENBURG, A., NERONOV, A. & VAZZA, F. 2024 Resistively controlled primordial magnetic turbulence decay. *Astron. Astrophys., in press* p. arXiv:2401.08569, arXiv: 2401.08569.
- BRANDENBURG, A., SHARMA, R. & VACHASPATI, T. 2023*b* Inverse cascading for initial magnetohydrodynamic turbulence spectra between Saffman and Batchelor. *J. Plasma Phys.* **89** (6), 905890606, arXiv: 2307.04602.
- BURROWS, A. & LATTIMER, J. M. 1986 The Birth of Neutron Stars. *Astrophys. J.* **307**, 178.
- CHRISTENSSON, M., HINDMARSH, M. & BRANDENBURG, A. 2001 Inverse cascade in decaying three-dimensional magnetohydrodynamic turbulence. *Phys. Rev. E* **64**, 056405.
- DAVIDSON, P. A. 2000 Was Loitsyansky correct? A review of the arguments. *Journal of Turbulence* **1** (1), 6.
- EPSTEIN, R. I. 1979 Lepton-driven convection in supernovae. *Mon. Not. R. Astron. Soc.* **188**, 305–325.
- FRISCH, U., POUQUET, A., LEORAT, J. & MAZURE, A. 1975 Possibility of an inverse cascade of magnetic helicity in magnetohydrodynamic turbulence. *J. Fluid Mech.* **68**, 769–778.
- GUILLET, J., REBOUL-SALZE, A., RAYNAUD, R., BUGLI, M. & GALLET, B. 2022 MRI-driven dynamo at very high magnetic Prandtl numbers. *Mon. Not. R. Astron. Soc.* **516** (3), 4346–4353, arXiv: 2205.08602.
- HATORI, T. 1984 Kolmogorov-Style Argument for the Decaying Homogeneous MHD Turbulence. *J. Phys. Soc. Jpn* **53** (8), 2539.
- HOSKING, D. N. & SCHEKOCHIHIN, A. A. 2021 Reconnection-Controlled Decay of Magnetohydrodynamic Turbulence and the Role of Invariants. *Phys. Rev. X* **11** (4), 041005, arXiv: 2012.01393.
- HOSKING, D. N. & SCHEKOCHIHIN, A. A. 2023*a* Cosmic-void observations reconciled with primordial magnetogenesis. *Nat. Comm.* **14**, 7523, arXiv: 2203.03573.
- HOSKING, D. N. & SCHEKOCHIHIN, A. A. 2023*b* Emergence of long-range correlations and thermal spectra in forced turbulence. *Journal of Fluid Mechanics* **973**, A13, arXiv: 2202.00462.
- Ji, HANTAO 1999 Turbulent Dynamos and Magnetic Helicity. *Phys. Rev. Lett.* **83** (16), 3198–3201, arXiv: astro-ph/0102321.
- KAHNIASHVILI, TINA, BRANDENBURG, AXEL, TEVZADZE, ALEXANDER G. & RATRA, BHARAT 2010 Numerical simulations of the decay of primordial magnetic turbulence. *Phys. Rev. D* **81** (12), 123002, arXiv: 1004.3084.
- KAHNIASHVILI, T., TEVZADZE, A. G., BRANDENBURG, A. & NERONOV, A. 2013 Evolution of primordial magnetic fields from phase transitions. *Phys. Rev. D* **87** (8), 083007, arXiv: 1212.0596.
- PARKER, E.N. 1955 Hydromagnetic dynamo models. *Astrophys. J.* **122**, 293–314.
- PENCIL CODE COLLABORATION, BRANDENBURG, A., JOHANSEN, A., BOURDIN, P., DOBLER, W., LYRA, W., RHEINHARDT, M., BINGERT, S., HAUGEN, N., MEE, A., GENT, F., BABKOVSKAIA, N., YANG, C.-C., HEINEMANN, T., DINTRANS, B., MITRA, D., CANDELAESI, S., WARNECKE, J., KÄPYLÄ, P., SCHREIBER, A., CHATTERJEE, P., KÄPYLÄ, M., LI, X.-Y., KRÜGER, J., AARNES, J., SARSON, G., OISHI, J., SCHOBER, J., PLASSON, R., SANDIN, C., KARCHNIWY, E., RODRIGUES, L., HUBBARD, A., GUERRERO, G., SNODIN, A., LOSADA, I., PEKKILÄ, J. & QIAN, C. 2021 The Pencil Code, a modular MPI code for partial differential equations and particles: multipurpose and multiuser-maintained. *J. Open Source Software* **6** (58), 2807.
- SCHEKOCHIHIN, A. A. 2022 MHD turbulence: a biased review. *J. Plasma Phys.* **88** (5), 155880501.
- TEVZADZE, A. G., KISSLINGER, L., BRANDENBURG, A. & KAHNIASHVILI, T. 2012 Magnetic Fields from QCD Phase Transitions. *Astrophys. J.* **759**, 54, arXiv: 1207.0751.
- THOMPSON, C. & DUNCAN, R. C. 1993 Neutron Star Dynamos and the Origins of Pulsar Magnetism. *Astrophys. J.* **408**, 194.
- YOUSEF, T. A. & BRANDENBURG, A. 2003 Relaxation of writhe and twist of a bi-helical magnetic field. *A&A* **407**, 7–12, arXiv: astro-ph/0303148.
- ZHOU, H., SHARMA, R. & BRANDENBURG, A. 2022 Scaling of the Hosking integral in

decaying magnetically dominated turbulence. *J. Plasma Phys.* **88** (6), 905880602, arXiv: 2206.07513.

ZRAKE, J. 2014 Inverse cascade of nonhelical magnetic turbulence in a relativistic fluid. *Astrophys. J. Lett.* **794** (2), L26, arXiv: 1407.5626.